

GRAVITATIONAL WAVE MEMORY FROM A PROPAGATING RELATIVISTIC JET: A PROBE TO THE INTERIOR OF GAMMA-RAY BURST PROGENITORS

YUN-WEI YU^{1,2}*Draft version December 21, 2024*

ABSTRACT

It is believed that the relativistic jets of gamma-ray bursts (GRBs) should initially propagate through a heavy envelope of the massive progenitor stars or through a merger ejecta formed from the compact binary mergers. The interaction of a jet with a stellar envelope or a merger ejecta can lead to the deceleration of the head material of the jet and, simultaneously, the formation of a hot cocoon. However, this jet-envelope/ejecta interaction is actually undetectable with electromagnetic radiation and can only be inferred indirectly by the structure of the breakout jet. Therefore, as a way out of this difficulty, it is suggested that the jet-envelope/ejecta interaction can produce a gravitational wave memory of an amplitude of $h \sim 10^{-27} - 10^{-24}$, which could be detected with some future gravitational wave detectors sensitive in the frequency range of $f \sim 0.1 - 1$ Hz. This provides a potential direct way to probe the jet propagation and then the interior of the GRB progenitors. Moreover, this method is in principle available even if the jet is finally choked in the stellar envelope or the merger ejecta.

Subject headings: gamma-ray bursts — gravitational waves — relativistic jets

1. INTRODUCTION

Relativistic jets are widely believed to be driven by the engines of gamma-ray bursts (GRBs). Such a jet should cross through a dense medium and be collimated there before it generates the GRB emission. Specifically, for long-duration GRBs originating from the core-collapse of massive stars (Woosley 1993; Woosley & Heger 2006; Galama et al. 1998; Stanek et al. 2003; Hjorth et al. 2003), the medium involved is just the heavy envelope of the massive progenitors. For short-duration GRBs created by the mergers of compact binaries (Paczynski 1986; Eichler et al. 1989; Narayan et al. 1992; Abbott et al. 2017), the dense medium surrounding the merger products can be contributed by various material ejections during the mergers (see Shibata & Hotokezaka (2019) for a review). The interaction between the GRB jet and the envelope/ejecta can in principle provide plenty of information about the density profile of the envelope/ejecta. The uncovering of the interior of GRB progenitors is one of the primary purposes of GRB researches. However, unfortunately, this jet-envelope/ejecta interaction is in fact unobservable only with electromagnetic waves, because the envelope/ejecta is very opaque.

An indirect clue to the jet propagation could be found from the structures of the observable jet and cocoon that have broken out from the envelope/ejecta, although it is still not easy to infer these structures by using the observations of the GRB prompt and afterglow emissions. Recently, a very special opportunity had appeared in the joint observation of a gravitational wave (GW) event GW170817 and a short GRB 170817A (Abbott et al. 2017; Goldstein et al. 2017). On the one hand, the GW detection robustly indicated that the line of sight of this event significantly deviates from the normal direction of

the orbital plane of the merging binaries and thus deviates from the symmetric axis of the GRB outflow. On the other hand, tremendous interest has been successfully generated by the GW detection, leading to a very wide champion of follow-up observations. As a result, the host galaxy, the associated kilonova, and the multi-wavelength afterglow emissions of GRB 170817A had been discovered subsequently and been monitored carefully and lastingly (Coulter et al. 2017; Hallinan et al. 2017; Troja et al. 2017). The prompt and afterglow emissions strongly suggested that the jet of GRB 170817A is highly structured. Its energy and velocity can decrease quickly with the increasing angle relative to the jet axis, which leads to the extremely low luminosity of GRB 170817A (Goldstein et al. 2017; Zhang et al. 2018). Therefore, in principle, the jet structure can be constrained by the dependence of the GRB event rates on their luminosities, although which is very difficult because of the high uncertainty of the intrinsic luminosity function of the GRB jets (Gupte & Bartos 2018; Salafia et al. 2019; Tan & Yu 2019). More excitingly, for such an off-axis observed GRB, the angular distributions of the energy and Lorentz factor of the jet can even be directly derived from the afterglow light curves, because the lasting increase of the afterglow fluxes could just be due to that the line of sight becomes closer and closer to the core of the jet (Xiao et al. 2017; Mooley et al. 2018; Granot et al. 2018; Lyman et al. 2018; Lazzati et al. 2018; Ioka & Nakamura 2018). As implied, a GRB jet is very likely to consist of a relativistic narrow core and a mildly-relativistic wide-spreading wing. This jet structure undoubtedly offers a stringent constraint on the preceding interaction between the jet and the progenitor material.

Despite of the important implication from the jet structure, it is still very concerned whether we can probe the jet-envelope/ejecta interaction and the GRB progenitor interior more directly, in particular, in the rapidly developing era of GW astronomy. Therefore, it is recalled

¹ Institute of Astrophysics, Central China Normal University, Wuhan 430079, China, yuyw@mail.ccnu.edu.cn

² Key Laboratory of Quark and Lepton Physics (Central China Normal University), Ministry of Education, Wuhan 430079, China

that, when a particle changes its velocity v by interacting with other objects, the metric perturbation induced by this particle, $h \sim 4GE\beta^2/(c^4D)$, can change correspondingly, where G is the gravitational constant, E is the particle energy, $\beta = v/c$, c is the speed of light, and D is the luminosity distance of the particle to the observer. Consequently, a GW radiation can be generated as a response to this metric change (Segalis & Ori 2001). Such a GW signal arising from an unidirectional metric variation (i.e., the metric perturbation does not return to its original value) is strictly not a periodic “wave” but, instead, is usually called as a “memory” (Sago et al. 2004). The characteristic frequency of a GW memory is determined by the timescale of the velocity change. Following this consideration, some authors had investigated the GW memory generated by radiating GRB jets (Sago et al. 2004; Akiba et al. 2013; Birnholtz & Piran 2013).

We would like to further point out that the propagation of a GRB jet is just a lasting process of (i) the sharp deceleration of the jet material at its head and (ii) the acceleration and heating of the envelope/ejecta material. Therefore, a GW memory can be naturally expected to arise from these velocity jump processes. If detected, this GW memory can provide a direct probe to the jet-envelope/ejecta interaction, which can effectively help to determine the nature of the GRB progenitors. To be specific, by taking some reference density profiles for the envelope/ejecta material, this paper is devoted to calculate the characteristic amplitude and frequency of the GW memory due to the jet propagation in these material. The detectability of this GW memory will also be discussed.

2. THE DYNAMICS OF JET PROPAGATION

The dynamics of a relativistic jet propagating in an envelope/ejecta has been investigated widely by using both analytical and numerical methods (Matzner 2003; Bromberg et al. 2011; Levinson & Begelman 2013; Nakauchi et al. 2013; Nagakura et al. 2014; Bromberg et al. 2014; Bromberg & Tchekhovskoy 2016; Matsumoto & Kimura 2018; Geng et al. 2019; Hamidani et al. 2019). When a relativistic jet propagates into a medium, the collision between the jet and the medium can lead to a forward shock sweeping up the medium and a reverse shock accumulating jet material. The region between these two shocks can be called as the head of the jet. The hot material in the jet’s head flows quickly and laterally to form a cocoon surrounding the jet. Then the high pressure of the cocoon can drive a collimation shock in the jet material toward the jet axis. As a result, the jet can be gradually collimated until it breaks out from the medium.

Following the above consideration, the velocity of a jet head can be determined by balancing the ram pressures of the forward-shocked envelope/ejecta and the reverse-shocked jet (Matzner 2003; Matsumoto & Kimura 2018):

$$\beta_h = \frac{\beta_j \tilde{L}^{1/2} + \beta_e}{\tilde{L}^{1/2} + 1} \quad (1)$$

with $\tilde{L} \simeq L_j/(\Sigma_j \rho_e \Gamma_e^2 c^3)$, where $\beta_j \simeq 1$, L_j , and Σ_j are the velocity, one-sided luminosity, and cross section of the unshocked jet, respectively, and ρ_e , β_e , and Γ_e are

the density, velocity, and Lorentz factor of the circum material (i.e., the envelope/ejecta material), respectively.

The cross section of the jet can be calculated easily by

$$\Sigma_j = \pi \theta_{j0}^2 z_h^2, \quad (2)$$

if the jet collimation due to the cocoon pressure is weak and the jet keeps conical, where θ_{j0} is the initial opening angle of the jet at launch and $z_h = \int_0^t \beta_h c dt$ is the height of the jet head. Nevertheless, in fact, the collimation effect is significant, once the jet height exceeds a critical point at $\hat{z} \approx (L_j/\pi c P_c)^{1/2}$ where the collimation shock converges. The expression of \hat{z} can be derived from the geometry equation of the collimation shock front (Komissarov, & Falle 1997; Bromberg et al. 2011), where P_c is the ram pressure in the cocoon. Due to the collimation, the jet cross section should be determined alternatively by (Bromberg et al. 2011)

$$\Sigma_j = \pi \theta_{j0}^2 \left(\frac{\hat{z}}{2} \right)^2 \simeq \frac{\theta_{j0}^2 L_j}{4c P_c}, \quad (3)$$

where a height of $\hat{z}/2$ is used because, at this point, the jet shape starts to be transformed from conical to cylindrical. More specifically, at $\hat{z}/2$, the collimation shock becomes roughly parallel to the jet axis. In the following calculations, we use the smaller value by comparing Eqs. (2) and (3).

The pressure in the cocoon can be estimated by $P_c = E_c/(3V_c)$, by assuming it is radiation-dominated, where E_c is the total energy stored in the cocoon and V_c is the volume. By considering of the continuous energy injection from the jet head, the cocoon energy can be calculated by

$$E_c = \int_0^t L_j (1 - \beta_h) dt'. \quad (4)$$

The radius of the cross section of the cocoon is given by $r_c = \int_0^t \beta_c c dt'$, where the lateral expansion velocity reads $\beta_c = [P_c/\bar{\rho}_e(z_h)c^2]^{1/2}$ (Begelman & Cioffi 1989) and $\bar{\rho}_e = \int \rho_e(z) dV/V_c$ is the average density of the cocoon. Then, we can estimate the volume of the cocoon by $V_c = \pi r_c^2 z_h$, where the shape of the cocoon is simply assumed to be cylindrical.

The density profile of the circum material can be usually described approximately by a power law. To be specific, for long GRBs, we use

$$\rho_e(z) = \rho_{e,*} \left(1 + \frac{z}{z_*} \right)^{-\delta}, \quad \text{for } z \leq z_s \quad (5)$$

with $\rho_{e,*} = 2.4 \times 10^9 \text{ g cm}^{-3}$, $z_* = 10^8 \text{ cm}$, $\delta = 3.5$, and $z_s = 10^{11} \text{ cm}$, which correspond to a Wolf-Rayet star of a mass of $15M_\odot$ (Suwa & Ioka 2011). Here the stellar envelope is considered to be static with $\beta_e = 0$, by ignoring the relatively slow supernova expansion. For short GRBs, according to numerical simulations of binary neutron star mergers (Hotokezaka et al. 2013), the density profile of the merger ejecta can be written as

$$\rho_e(z) = \frac{(3-\delta)M_{ej}}{4\pi z_{\min}^3} \left[1 - \left(\frac{z_{\max}}{z_{\min}} \right)^{3-\delta} \right]^{-1} \left(\frac{z}{z_{\min}} \right)^{-\delta}, \quad \text{for } z_{\min} \leq z \leq z_{\max} \quad (6)$$

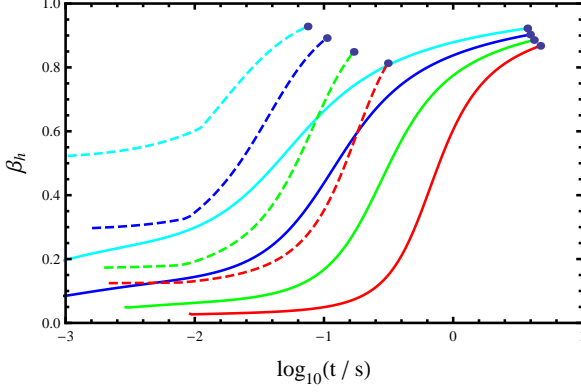


FIG. 1.— The evolution of the head velocity of a relativistic jet for different luminosities, i.e., $L_j = 10^{49}$, 10^{50} , 10^{51} , and $10^{52} \text{ erg s}^{-1}$ from bottom to top. The solid and dashed lines correspond to long and short GRBs, respectively. The thick points represent the breakout of the jet. The other parameters are declared in the text.

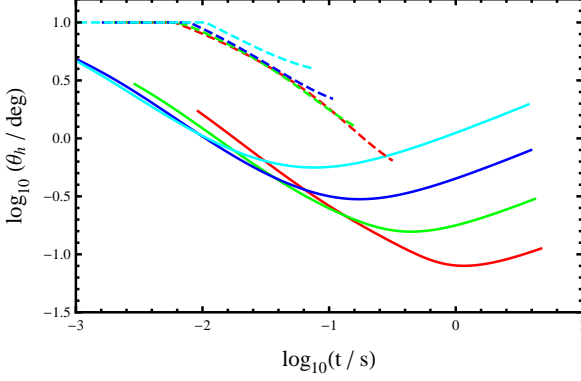


FIG. 2.— The evolution of the opening angle of the jet head relative to the central engine.

where $M_{\text{ej}} = 0.01 M_{\odot}$ is the total mass of the ejecta, $\delta = 3.5$, and $z_{\text{max}} = v_{\text{e,max}} t$ and $z_{\text{min}} = v_{\text{e,min}} t$ are given for $v_{\text{e,max}} = 0.4c$ and $v_{\text{e,min}} = 0.1c$ (Nagakura et al. 2014).

As addressed, the dynamical evolution of the jet propagation is primarily dependent on the numerical ratio between the energy flux of the jet and the density of the circum material. Therefore, in our calculations, we only take some reference density profiles and fix the initial opening angle to be $\theta_{j0} = 10^\circ$, while the value of L_j is varied within a wide range of $10^{49} - 10^{52} \text{ erg s}^{-1}$. Additionally, the luminosity is considered to not evolve with time. Then, we plot the velocity evolution of the jet head in Figure 1, for different jet luminosities. Meanwhile, we also plot in Figure 2 the evolution of the opening angle of the jet head relative to the central engine as defined by

$$\theta_h = \left(\frac{\Sigma_j}{\pi z_h^2} \right)^{1/2}, \quad (7)$$

from which we can see the degree of the jet collimation. It is showed that the edge of the jet is squeezed by the cocoon significantly and thus the jet material is pushed and accelerated. For both long and short GRBs, the higher the jet luminosity, the higher the head velocity and the shorter the time of the jet breakout.

3. THE GW MEMORY FROM A JET HEAD

The metric perturbation $h_{\mu\nu} = g_{\mu\nu} - \eta_{\mu\nu}$ induced by a point mass m of a four-velocity $u^\mu(\tau) = \gamma c(1, \vec{\beta})$ can be solved from the following linearized Einstein equation (under the Lorentz gauge condition) (Segalis & Ori 2001)

$$\left(-\frac{1}{c^2} \frac{\partial^2}{\partial t^2} + \Delta \right) \bar{h}_{\mu\nu} = -16\pi G T_{\mu\nu} \quad (8)$$

with the energy-momentum tensor

$$T^{\mu\nu}(x) = \int m u^\mu(\tau) u^\nu(\tau) \delta^{(4)}[x - x(\tau)] d\tau, \quad (9)$$

where $\bar{h}_{\mu\nu} \equiv h_{\mu\nu} - \frac{1}{2} \eta_{\mu\nu} h^\lambda_\lambda$, $\eta_{\mu\nu} = (-1, +1, +1, +1)$ is the Minkowski metric, and τ is the proper time. By setting the z -axis at the velocity direction and transforming $h_{\mu\nu}$ from the Lorentz gauge to the transverse-traceless (TT) gauge, the TT parts of h_{ij} read (Segalis & Ori 2001; Sago et al. 2004; Akiba et al. 2013)

$$h_+ \equiv h_{xx}^{\text{TT}} = -h_{yy}^{\text{TT}} = \frac{2GE}{c^4 D} \frac{\beta^2 \sin^2 \vartheta}{1 - \beta \cos \vartheta} \cos 2\varphi, \quad (10)$$

$$h_\times \equiv h_{xy}^{\text{TT}} = h_{yx}^{\text{TT}} = \frac{2GE}{c^4 D} \frac{\beta^2 \sin^2 \vartheta}{1 - \beta \cos \vartheta} \sin 2\varphi, \quad (11)$$

which are useful for calculating the response of a GW detector. Here a general expression of energy E is used to replace the original term γmc^2 , in order to take into account the metric perturbation induced by a hot moving material, e.g., shocked material.

In a differential solid angle of a relativistic GRB jet, an amount of energy $\dot{E}_c d\theta d\phi / \Omega_h$ can be transferred per second from the upstream of the reverse shock into the head region of the jet, where the spherical coordinates (θ, ϕ) are defined by setting the z -axis at the symmetric axis of the jet and $\Omega_h = 2\pi(1 - \cos \theta_h)$ is the total opening solid angle of the jet head that is given by Equation (7). Accompanying with this energy transfer, the velocity of the jet material varies from $\sim c$ to $c\beta_h(t)$, which therefore leads to a change of the metric perturbation. Then, by using Eqs. (10) and (11) and combining the contributions of all differential elements, the change rate of the metric perturbation due to a jet propagation can be given by

$$\dot{h}_+(t) = \frac{2G}{c^4 D} \frac{\dot{E}_c(t)}{\Omega_h} \int_0^{2\pi} \int_0^{\theta_h(t)} \sin \theta d\theta d\phi \times \left[\frac{\sin^2 \vartheta}{1 - \cos \vartheta} - \frac{\beta_h(t)^2 \sin^2 \vartheta}{1 - \beta_h(t) \cos \vartheta} \right] \cos 2\varphi, \quad (12)$$

$$\dot{h}_\times(t) = \frac{2G}{c^4 D} \frac{\dot{E}_c(t)}{\Omega_h} \int_0^{2\pi} \int_0^{\theta_h(t)} \sin \theta d\theta d\phi \times \left[\frac{\sin^2 \vartheta}{1 - \cos \vartheta} - \frac{\beta_h(t)^2 \sin^2 \vartheta}{1 - \beta_h(t) \cos \vartheta} \right] \sin 2\varphi. \quad (13)$$

For a viewing angle θ_v relative to the jet axis, the relationship between (ϑ, φ) and (θ, ϕ) can be written as Akiba et al. (2013)

$$\sin \vartheta \cos \varphi = -\sin \theta_v \cos \theta + \cos \theta_v \sin \theta \cos \phi, \quad (14)$$

$$\sin \vartheta \sin \varphi = \sin \theta \sin \phi, \quad (15)$$

$$\cos \vartheta = \cos \theta_v \cos \theta + \sin \theta_v \sin \theta \cos \phi. \quad (16)$$

Besides the reverse-shocked jet material, the energy injection into the head region represented by \dot{E}_c is also

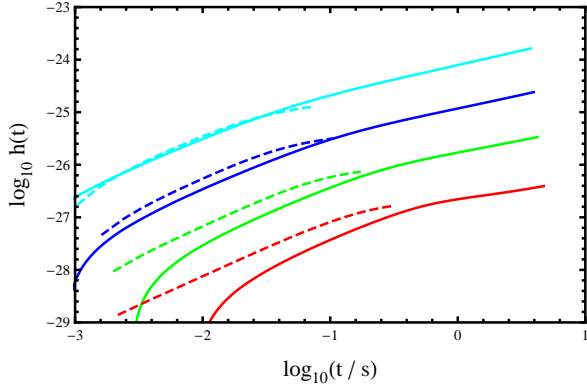


FIG. 3.— The increasing amplitude of the GW memory due to a jet propagation. A viewing angle $\theta_v = 15^\circ$ is taken. The reference distances of 50 and 130 Mpc are taken for the short and long GRBs, respectively.

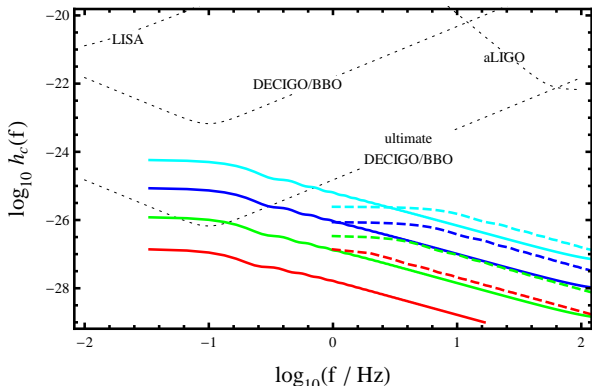


FIG. 4.— The characteristic amplitude of the GW memory as a function of the GW frequency. The dotted lines give the noise amplitude of the GW detectors as labeled.

highly shared by the forward-shocked medium. This means the h -variations presented in Equations (12) and (13) actually have included the contribution due to the mass flow from the unshocked medium into the jet head. Additionally, in contrast to the velocity difference between the jet and its head, the velocity can only change slightly as the material flows from the jet head into the surrounding cocoon. Therefore, the h -variation due to the latter process can be ignored. To be summarized, at a time of t , the amplitude of the GW memory arising from the jet propagation can be calculated by

$$h(t) = \sqrt{h_+(t)^2 + h_\times(t)^2}, \quad (17)$$

by integrating Equations. (12) and (13) over the time. To a good approximation, the change rate of h can be simply approximated by

$$\dot{h}(t) = \frac{2G\dot{E}_c(t)}{c^4 D} \left[\frac{\sin^2 \theta_v}{1 - \cos \theta_v} - \frac{\beta_h(t)^2 \sin^2 \theta_v}{1 - \beta_h(t) \cos \theta_v} \right], \quad (18)$$

if the viewing angle θ_v is not too small.

Determined by Eqs. (12) and (13), the GW memory radiation is anti-beamed, just as emphasized frequently in literature (Sago et al. 2004; Akiba et al. 2013; Birnholtz & Piran 2013). That is, the amplitude of the GW memory is nearly independent of the viewing angle, unless the observation is on-axis (i.e., θ_v is less than a few of degrees). On the contrary, the electromagnetic

emission from a relativistic GRB jet is highly beamed within an angle of $\theta \sim \Gamma_j^{-1}$. Therefore, the detection probability of a GW memory could be very much higher than that of its associated GRB emission. Furthermore, one should note that the GW memory radiation cannot be obstructed by the circum medium and thus it is detectable even though the jet is finally choked by the circum medium. Therefore, it seems reasonable to estimate the event rate of these GW memories by the total rate of GRBs without considering the beaming effect. To be specific, in the near universe where the memory can be detected, we can take roughly $\sim 100 \text{ Gpc}^{-3} \text{ yr}^{-1}$ for long GRBs (Wanderman, & Piran 2010; Cao et al. 2011) and $\sim 1500 \text{ Gpc}^{-3} \text{ yr}^{-1}$ for short GRBs (Abbott et al. 2017). According to these local event rates, we can further determine a reference distance, within which about one GRB can happen in one year. It is $\sim 130 \text{ Mpc}$ and $\sim 50 \text{ Mpc}$ for long and short GRBs, respectively. For these distances, we present the increasing amplitudes of the GW memories in Figure 3, where a viewing angle $\theta_v = 15^\circ$ is taken. The profiles of these lines are determined completely by the jet luminosity and the dynamical evolution of the jet propagation. Therefore, it can help us to shed light into these physical processes occurring inside GRB progenitors.

For a comparison with the noise amplitude of some GW detectors, we calculate the characteristic amplitude of a GW memory by

$$h_c(f) = 2f|\tilde{h}| \equiv 2f \left| \int_{-\infty}^{\infty} h(t) \exp(i2\pi ft) dt \right|, \quad (19)$$

where f is the GW frequency. The obtained results are presented in Figure 4. Here, limited by the resolution of the used fast fourier transform, these amplitude lines could only give the envelope of rapidly oscillating lines, where a plenty of oscillations could not be exhibited in details. In any case, it is showed that the characteristic frequencies of the GW memories are primarily around $\sim 0.1 \text{ Hz}$ for long GRBs and $\sim 1 \text{ Hz}$ for short GRBs, which correspond to the typical timescales of the jet breakout of a few seconds and a few tenths of seconds (see Figure 1), respectively. In Figure 4, the noise amplitudes of the GW detectors are defined by $h_n(f) = [5fS_h(f)]^{1/2}$ as in (Sago et al. 2004). The expressions of the spectral density of the strain noise $S_h(f)$ for aLIGO, LISA, and DECIGO/BBO and as well as its ultimate value are taken from (Finn & Thorne 2000; Seto et al. 2001). In comparison, we find that the GW memories due to the jet propagation of long GRBs are very promising targets for DECIGO/BBO at its ultimate sensitivity, both in their characteristic amplitudes and frequencies. On the contrary, those from short GRBs could be difficult to be discovered with these GW detectors.

4. SUMMARY AND DISCUSSIONS

The GW memory from a relativistic GRB jet propagating into a dense circum material is investigated, where the circum medium specifically corresponds to a stellar envelope or a merger ejecta. The characteristic frequency and amplitude of the GW memory are found to be potentially detectable with the future GW detectors such DECIGO/BBO at its ultimate sensitivity, in particular, for long GRBs. The detection of these GW memories

will provide a practicable method to probe the interior of the GRB progenitors, because the characteristic features of these memories are completely determined by the energy release of the GRB engines and the propagation dynamics of the relativistic jet. The combination of the GW memory detection with the off-axis observed GRB prompt and afterglow emissions can further yield a stringent constraint on the interaction between the jet and the circum material.

In principle, a relativistic jet has a large opportunity to be choked by the circum material. Then, a GRB emission would be unexpected, other than a gamma-ray/X-ray flash possibly arising from the hot cocoon. So, the jet-progenitor interaction definitely cannot be inferred by constraining the jet structure by using GRB observations. However, fortunately, the GW memory predicted in this paper is always detectable. Despite of the absence of the GRB emission, for sufficiently small distances at which the memory can be detected, a nearly isotropic

supernova/kilonova emission can still be expected to accompany with the memory signal. Then, these optical transients can be used to effectively localize and calibrate the memory signal. At the same time, the GW memory can conversely help to identify the special origins of these optical transients, which are associated with a failed GRB. Additionally, it is worth mentioning that the propagating GRB jets can also be detected through high-energy neutrinos, which can be produced by the internal and collimation shocks in the jets (Horiuchi & Ando 2008; Kimura et al. 2018). These future multi-messenger observations can undoubtedly help to extend and complete our understanding of the GRB phenomena, in particular, of the interior of different GRB progenitors.

This work is supported by the National Natural Science Foundation of China (Grant Nos. 11822302 and 11833003) and the Fundamental Research Funds for the Central Universities (Grant No. CCNU18ZDPY06).

REFERENCES

- Abbott, B. P., Abbott, R., Abbott, T., et al. 2017, PRL, 119, 161101
- Akiba, S., Nakada, M., Yamaguchi, C., et al. 2013, PASJ, 65, 59
- Begelman, M. C., & Cioffi, D. F. 1989, ApJ, 345, L21
- Birnholtz, O., & Piran, T. 2013, Phys. Rev. D, 87, 123007
- Bromberg, O., Nakar, E., Piran, T., et al. 2011, ApJ, 740, 100
- Bromberg, O., & Tchekhovskoy, A. 2016, MNRAS, 456, 1739
- Bromberg, O., Granot, J., Lyubarsky, Y., et al. 2014, MNRAS, 443, 1532
- Cao, X.-F., Yu, Y.-W., Cheng, K. S., et al. 2011, MNRAS, 416, 2174
- Coulter, D. A., Foley, R. J., Kilpatrick, C. D., et al. 2017, Science, 358, 1556
- Eichler, D., Livio, M., Piran, T. & Schramm, D. N. 1989, Nature, 340, 126
- Finn, L. S., & Thorne, K. S. 2000, Phys. Rev. D, 62, 124021
- Galama, T. J., Vreeswijk, P. M., van Paradijs, J., et al. 1998, Nature, 395, 670
- Geng, J.-J., Zhang, B., Kölligan, A., et al. 2019, ApJ, 877, L40
- Goldstein, A., Veres, P., Burns, E., et al., 2017, ApJL, 848, L14
- Granot, J., Gill, R., Guetta, D., et al. 2018, MNRAS, 481, 1597
- Gupte, N., & Bartos, I. 2018, arXiv e-prints, arXiv:1808.06238
- Hallinan, G., Corsi, A., Mooley, K. P., et al. 2017, Science, 358, 1579
- Hamidani, H., Kiuchi, K., & Ioka, K. 2019, arXiv e-prints, arXiv:1909.05867
- Horiuchi, S., & Ando, S. 2008, Phys. Rev. D, 77, 063007
- Hjorth, J., Sollerman, J., Møller, et al., 2003, Nature, 423, 847
- Hotokezaka, K., Kiuchi, K., Kyutoku, K., et al. 2013, Phys. Rev. D, 87, 024001
- Ioka, K., & Nakamura, T. 2018, Progress of Theoretical and Experimental Physics, 2018, 043E02
- Kimura, S. S., Murase, K., Bartos, I., et al. 2018, Phys. Rev. D, 98, 043020
- Komissarov, S. S., & Falle, S. A. E. G. 1997, MNRAS, 288, 833
- Lazzati, D., Perna, R., Morsony, B. J., et al. 2018, Phys. Rev. Lett., 120, 241103
- Levinson, A., & Begelman, M. C. 2013, ApJ, 764, 148
- Lyman, J. D., Lamb, G. P., Levan, A. J., et al. 2018, Nature Astronomy, 2, 751
- Matsumoto, T., & Kimura, S. S. 2018, ApJ, 866, L16
- Matzner, C. D. 2003, MNRAS, 345, 575
- Mooley, K. P., Nakar, E., Hotokezaka, K., et al. 2018, Nature, 554, 207
- Nagakura, H., Hotokezaka, K., Sekiguchi, Y., et al. 2014, ApJ, 784, L28
- Nakauchi, D., Kashiya, K., Suwa, Y., et al. 2013, ApJ, 778, 67
- Narayan, R., Paczyński, B., Piran, T., 1992, ApJL, 395, L83
- Paczynski, B., 1986, ApJL, 308, L43
- Sago, N., Ioka, K., Nakamura, T., et al. 2004, Phys. Rev. D, 70, 104012
- Salafia, O. S., Barbieri, C., Ascenzi, S., et al. 2019, arXiv e-prints, arXiv:1907.07599
- Segalis, E. B., & Ori, A. 2001, Phys. Rev. D, 64, 064018
- Seto, N., Kawamura, S., & Nakamura, T. 2001, Phys. Rev. Lett., 87, 221103
- Shibata, M., & Hotokezaka, K. 2019, Annual Review of Nuclear and Particle Science, 69, annurev
- Stanek, K. Z., Matheson, T., Garnavich, P., et al., 2003, ApJL, 591, L17
- Suwa, Y., & Ioka, K. 2011, ApJ, 726, 107
- Tan, W.-W., & Yu, Y.-W. 2019, ApJ, submitted
- Troja, E., Piro, L., van Eerten, H., et al. 2017, Nature, 551, 71
- Wanderman, D., & Piran, T. 2010, MNRAS, 406, 1944
- Woosley S. E., 1993, ApJ, 405, 273
- Woosley S. E., Heger A., 2006, ApJ, 637, 914
- Xiao, D., Liu, L.-D., Dai, Z.-G., et al. 2017, ApJ, 850, L41
- Zhang, B.-B., Zhang, B., Sun, H., et al. 2018, Nature Communications, 9, 447